

68th Conference of the Italian Thermal Machines Engineering Association, ATI2013

Vapour - Liquid Equilibrium measurements of CO₂ based mixtures: experimental apparatus and testing procedures

Silvia Lasala^{a,*}, Paolo Chiesa^a, Daniele Di Bona^{a,b}, Stefano Consonni^{a,b}

^aPolitecnico di Milano – Department of Energy – Via Lambruschini 4, 20156 Milano, Italy

^bLEAP – Via Nino Bixio 27, 29121 Piacenza, Italy, www.leap.polimi.it

Abstract

At present, the accurate evaluation of the thermo-physical behaviour of multicomponent fluids represents a crucial element for studying and simulating low CO₂ emission energy conversion technologies. In order to extend the range of application of the available thermodynamic models, an intense experimental research activity has been performed in recent years. The main purpose of this paper is to describe the experimental and modelling procedures applied by the authors to measure and to analyse data extracted from the Vapour-Liquid Equilibrium apparatus recently installed at LEAP laboratory. This test rig allows the characterization of mixture phase equilibrium properties on the basis of the static-analytical method, within the pressure and temperature ranges of 0 – 20 MPa and -60 – 200 °C. Finally, the paper reports the most relevant features and the main guidelines for the instruments calibration procedures.

© 2013 The Authors. Published by Elsevier Ltd.

Selection and peer-review under responsibility of ATI NAZIONALE

Keywords: Vapor-Liquid Equilibrium measurements; carbon dioxide; closed-cycle working fluid; mixture.

1. Motivation

During the last decade, concerns regarding the need of stabilizing the greenhouse gases concentration in the atmosphere have supported the growth of low CO₂ emission technologies for energy conversion.

In particular, closed-cycle power plants such as Organic Rankine Cycles (ORCs) and carbon dioxide Brayton and Rankine cycles are widely recognized as an attractive option for medium capacity energy conversion systems [1-6]. The introduction of Rankine cycles based on organic fluids, instead of water, has allowed the exploitation of several

* Corresponding author. Tel.: +39-0523-35-6824.
E-mail address: silvia.lasala@polimi.it

low-temperature energy sources, such as solar, geothermal and biomass ones. Being based on the well-known steam-water cycle technology, the ORC is currently a widely spread form of energy production. On the other hand, supercritical carbon dioxide closed-cycles offer the potential of equivalent or higher cycle efficiency compared to supercritical or superheated steam cycles at temperatures relevant for nuclear, solar and geothermal energy conversion systems [7]. The most important innovation introduced by these closed cycles is the possibility of varying their working fluid, considered as a further degree of freedom. Up to now, only pure fluids have been employed but it is also being evaluated the possibility of using mixtures. In fact, it has been widely attested that performance and flexibility of both these cycles can be improved by adopting multicomponent fluids [8]. The use of mixtures as ORC working fluids can be extremely attractive when both hot and cold sinks are characterized by variable temperature profiles. Indeed, mixture temperature glides arising during condensation and evaporation would maximize the heat exchanges effectiveness thus resulting in an improved efficiency. In the case of CO₂ gas cycle, the increase of pure CO₂ critical temperature by the addition of some specific components would greatly improve the efficiency of the cycle itself, benefitting from the advantages of carbon dioxide real gas effects [9].

Another important option for the reduction of CO₂ emissions is represented by carbon dioxide capture and storage (CCS) technologies. Thorough studies are being dedicated to the optimal design of these processes. Nevertheless, some issues still need to be addressed. In fact, depending on the fuel conversion process and on the applied carbon dioxide capture technology, different types and quantities of impurities are included in the captured CO₂ streams [10,11]. The current major difficulty consists of evaluating the modification of the thermodynamic behaviour of these CO₂ streams caused by the presence of such impurities.

On the basis of the above considerations, it can be stated that the challenge of improving the efficiency of low emissions energy processes requires an in-depth analysis of the thermo-physical properties of multicomponent fluids. Nonetheless, the lack of an equation of state being valid for all fluids at any temperature and pressure has entailed the necessity of defining thermodynamic models for each specific application, for which the minimum required accuracy level is only achievable by calibrating semi-empirical models on experimental data [12].

The purpose of the research activity undertaken from LEAP laboratory [13-17] is to investigate the thermodynamics of those particular fluids which could be relevant for the development of low CO₂ emission power technologies. Therefore, as an integration of what was described in [13], this paper aims to present the testing and modelling procedures applied from the authors to experiment with the VLE apparatus recently installed at LEAP.

2. Experimental apparatus

This section introduces the features of the experimental apparatus used at LEAP to perform vapour-liquid equilibrium measurements. The basic equipment has been designed and manufactured in 2012 by “ARMINES, Centre of Thermodynamics and Processes”, established at MINES ParisTech.

This phase equilibrium test rig, schematically represented in Fig.1, enables the measurement of VLE thermodynamic properties (P, T, x, y) of different fluids based on CO₂, N₂, O₂, CO, H₂S, SO₂, Ar, CH₃OH, ORC working fluids and refrigerants. Temperature and pressure operating conditions range respectively from 213 K to 473 K and from 10 bar to 199 bar.

The apparatus is based on a static-analytical method [18,19], therefore coexisting phases remain inside the cell during measurements (static method) and compositions of both liquid and vapour phases are determined by sampling and then by analysing them (analytical method).

With reference to Figure 1 and Table 1, the apparatus consists of a measurement circuit and two systems for loading, respectively, liquid and gaseous components in the equilibrium cell. In particular, the measurement circuit is composed by:

- pressure and temperature measurement devices (1a-1e, 2a-2e);
- a cell in which vapour and liquid phases of the mixture are in equilibrium (4);
- a sampling device for withdrawing vapour and liquid samples from the cell (6, 7);
- a gas chromatograph for measuring samples composition (8);
- a thermostatic bath that controls temperature of the equilibrium cell (12);

A detailed description of these components will be given in section 2.1. Moreover, section 2.2 delineates features of the loading circuits.

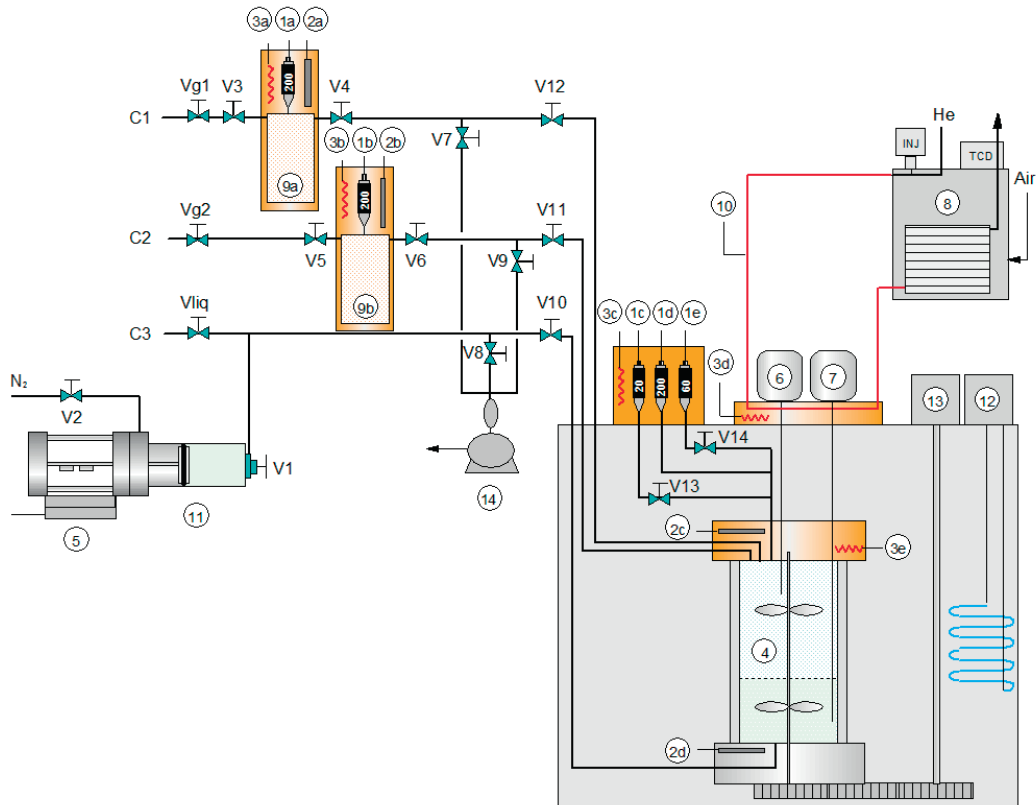


Fig. 1. Schematic of the VLE apparatus.

Table 1. Notation of the apparatus components shown in Fig. 1.

Notation	Component	Notation	Component
1a-1e	Pressure transducers	12	Thermostatic bath control system
2a-2d	100 ohm platinum probes	13	Stirrer electrical motor
3a-3e	Temperature regulators	14	Vacuum pump
4	Equilibrium cell	TCD	GC Thermal conductivity detector
5	Optoelectronic displacement rule	INJ	Injector
6	ROLSI liquid phase	C1	Component n. 1 (gas)
7	ROLSI vapour phase	C2	Component n. 2 (gas)
8	Gas chromatograph (GC)	C3	Component n. 3 (liquid or gas)
9	Gas tank	V1-V14	Valves
10	Thermo regulated sample transfer line	Vg	Gas loading valve
11	Liquid loading volume	Vliq	Liquid loading valve

2.1. Vapour – Liquid Equilibrium cell and sampling devices

Since it has been attested that the accuracy of results can be improved by adopting small-volume equilibrium environments [20-22], the cell has been specifically designed in order to fulfil this requirement. In fact, the measurement cell consists of a monocrystalline sapphire tube with an internal volume of approximately 34 cm³ (see Fig. 2).

However, equilibrium cells characterized by a reduced cell volume could involve the unwanted reduction of pressure during vapour and liquid phase sampling. To avoid this situation, proper sampling devices have been employed to allow the withdrawal of a minimum sampled volume (50 – 500 µl) with respect to the interior volume of the cell. To this end, liquid and vapour samples are extracted from the cell by two electromagnetic Rapid – Online – Sampler – Injector (ROLSI™) samplers (see Fig. 3) [23]. During the operating conditions, each ROLSI is crossed by a constant flow of carrier gas coming from the gas chromatograph front inlet. The side of the capillary connected to the sampler body is sealed by a mobile part whose upper and lower extremities consist of, respectively, a polymer part and a soft iron core, the latter being constrained by a spring. Samples are withdrawn by the action of an electromagnet which attracts the mobile part and opens the seal between the fixed capillary and the mobile part. The pressure inside the cell is higher than that in chromatographic circuit and, therefore, the sample flows through the stem of the sampling valve. After the sampling valve is closed, the sample is taken out by the carrier gas up to gas chromatograph. The amount of the withdrawn sample depends on pressure and temperature conditions and it is directly proportional to the seal opening time. An electrical power supply is connected to a digital timer Omron - H5CX, which allows the control of both the time between each sample withdrawal (time *t1*) and the ROLSI opening time (time *t2*). Once extracted, samples are heated in the expansion chamber of the ROLSI to completely vaporise the liquid samples and then transferred to the gas chromatograph column head through a thermally regulated transfer line. These temperature are set according to the specific analysed mixture, in order to avoid any product condensation along its transfer.

The temperature of the measurement cell is set using a LAUDA Kyromat RP 3090 thermostatic bath. Condensation and evaporation phenomena, that cause heat losses in the upper part of thermostatic bath, are minimized by a PTFE insulated plate adapted to the opening of the bath. This cover, connected to the equilibrium cell, can be raised by a dedicated electrical motor.

Two flanges of titanium TA6V connect, respectively, the upper and the lower bases of the cell tube to the rest of the circuit. The upper flange is equipped by a cartridge heater located inside a drilled well. This is needed to guarantee the isothermal environment along the cell, compensating for the unavoidable bath thermal losses which affect high temperature measurements.

A stirrer has been included in the cell to ensure the homogeneity of the mixture composition. It consists of a titanium magnetic rod positioned on a shaft with two propellers, driven by a variable speed motor.

The cell is loaded and drained through the use of three non-rotating loading needle valves (V10, V11, V12 in Fig. 1 and Fig. 2) specifically designed to avoid dead volumes. Two of them are connected to the cell through the upper flange and allow the entering of fluids in the gas phase. The third mentioned valve, located within the lower flange, is needed to introduce components in the liquid phase. Each of these three valves is connected upstream to a three way valve (V7, V8, V9 in Fig. 1), needed to create the vacuum inside the circuit. These three-way valves link, in turn, the measurement circuit to the loading one. The latter consists of two gas tanks and a variable volume press used, respectively, to load gaseous and liquid components. More details about the loading procedure will be given in section 2.2.

Cell temperature measurements are performed by Pt-100 probes inserted in both the upper and lower flanges. Pressure inside the cell is measured by three pressure sensors. They are connected to the upper flange of the cell through a 1/16" tube made of Hastelloy C276 and located inside a titanium support block positioned on the bath cover. Moreover, this block is thermostatically controlled by two cartridge heaters, each one equipped with a J-thermocouple and controlled by a FUJI PRX4 temperature regulator (see Fig. 1).

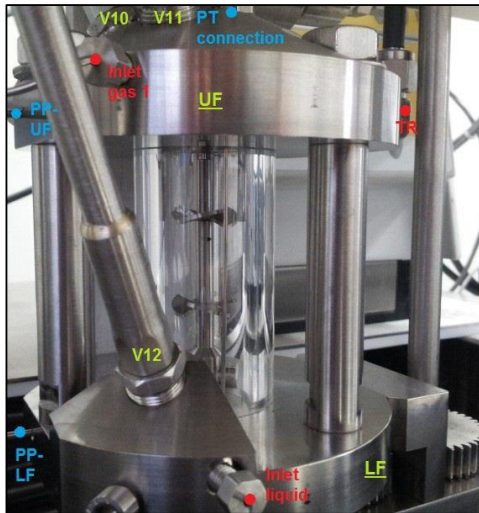


Fig. 2. Equilibrium cell.

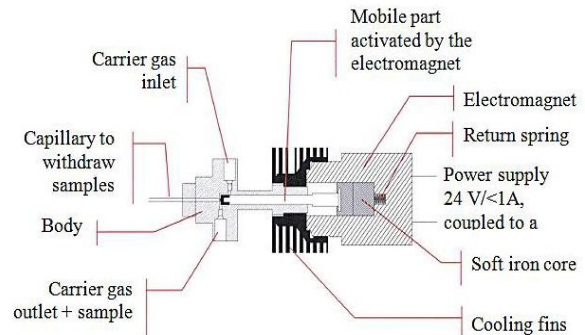


Fig. 3. Schematic of ROLSI™ Sampler injector.

2.2. Fluids loading systems

Mixtures are created inside the equilibrium cell by loading each component with a sequential order dictated by their relative volatility. Components can be loaded inside the cell in a liquid or gaseous phase through two different loading systems.

The liquid loading system consists of a variable volume press composed by a titanium cylindrical body and a piston sealed through a polymer o-ring. The piston separates the component to be loaded in the cell from the pressuring gas. The maximum volume of the cylinder which can be occupied by the loading fluid is around 100 cm³. Furthermore, the front part of this press has a non-rotating needle valve which is used for two purposes. Firstly, to load fluids by gravity from their storage tank into the press, after having created vacuum condition. Secondly, for the transferring of these loaded fluids into the measurement cell, in the liquid phase.

The variable volume press content is pressurized by a high pressure gas (nitrogen) acting on the piston. The amount of fluid loaded into the cell is controlled by measuring the longitudinal displacement of the piston, driven by the action of the pressurizing gas. This measurement is carried out with an optical rule (Heidenhain). The press has a rear flange fitted on the support part of the optical rule, which includes a valve that connects the nitrogen tank to the pressurizing side of the press. According to the manufacturer, the accuracies of the optical rule are $\pm 0.6 \mu\text{m}$.

The knowledge of the exact internal diameter of the press (34.99 mm \pm 0.02 mm) and the measurement of the piston displacement enables the computation of the loaded amount of fluid inside the cell. It must be highlighted that the straightforward relation between computed fluid volume variation and introduced moles of component is valid just in case the volume is filled with pure liquid phase. Hence, the value of the pressure for pressurization must be higher than the saturation pressure of the loaded fluid at the temperature of the environment where the press is located (usually ambient temperature).

Gaseous components can be loaded from two gas reserves, made of titanium, each of them consisting of a thermally insulated cylinder with an internal diameter of 45 mm and a height of 145 mm. The volume is approximately 230 cm³.

Each gas cylinder is connected through two stainless steel 316L valves to the circuit leading to the measurement cell and to the gas bottle where gas is stored. The upper part of the flange also includes a 200 bar pressure sensor GE Sensing UNIK 5000, a 100 ohm platinum probes class A and two cartridge heaters whose temperature is regulated.

The maximum temperature of the gas reserve is fixed at 75°C. The volume of each gas tank needs to be accurately calibrated as well as the loading circuit up to the inlet valve of the cell. Once this volume is known, the calculation of the introduced moles of gas can be performed, in isothermal condition, by measuring pressure inside the gas tank before and after the introduction of gas in the equilibrium cell.

3. Pressure, temperature and mixture composition measurements

3.1. Pressure and temperature

Pressure inside the cell is measured by three absolute pressure transmitters GE Sensing UNIK 5000 which range 2MPa, 6MPa and 20 MPa. Depending on the measured pressure, the two low pressure sensors may be isolated by using two non-rotating needle valves (V13 and V14 in Fig. 1). Pressure probes are calibrated in the pressure ranges 1–20MPa, in LEAP laboratory with a dead weight pressure balance (Scandura, Series MPA-R). The procedure followed for the calibration is the one suggested by ENV 13005 [24]. This calibration procedure also combines the uncertainty of the balance, periodically measured by Scandura and corrected for operating conditions at LEAP (local temperature, sensor position and local gravity) during probes calibration. During calibration, temperature of the heated support where pressure transducers are located is set to 60°C. The same temperature is maintained when performing measurements to avoid the influence of temperature variations in the measured pressure value. By keeping pressure transducers mounting at 60°C, the last calibration has shown an uncertainty on pressure measurements lower than $\pm 0.03\%$ of the read value in all the considered pressure ranges.

The temperature of the environment inside the cell is measured using two sheathed class A Pt-100 probes. As mentioned in the previous paragraph, these sensors are housed in the upper and lower flanges of the cell. The temperature gradient indicated by the two probes should be checked and minimized, in order to guarantee an homogeneous temperature along the cell. However, a slightly higher temperature (+0.1K) measured in the upper flange would prevent any condensation problem at the top of the cell. The maximum difference which could be accepted between these two readings is 0.3K and the average value between them is referred to as the equilibrium temperature. Temperature sensors are calibrated by an accredited calibration laboratory (LAT) of Politecnico di Milano. The estimated uncertainty is lower than 0.08K.

The output of each probe is acquired by a 34970A Agilent data acquisition unit.

3.2. Mixture composition

As described in section 2.1, accurate sampling of the vapour and liquid phase is carried out by two dedicated ROLSI. After being transferred to the gas chromatograph (Agilent 7820A), samples are processed by proper columns and analysed by a thermal conductivity detector. At present, helium is used as carrier gas.

Figures 4a and 4b show two configurations of the connections between the three capillary columns positioned inside the GC oven. Both the schemes show three columns and two rotating valves. In particular, Column 1 is a 0.53 mm ID, 25 m length PoraPLOT Q, while column 2 and 3 are both Molsieve 5A PLOT with a 0.53 mm ID and lengths of, respectively, 50 m and 25 m. The two valves have been installed in order to bypass column 1 or the series of column 2 and 3. The first valve enables the inlet of an external sample inside the circuit, while the second valve is necessary to avoid the contamination of the Molsieve columns (Col2 and Col3). In fact, Molsieve columns can only be crossed by light gases (oxygen, nitrogen, methane and carbon monoxide) and inert gases (helium, argon, neon, krypton and xenon). Also, they show an excellent effectiveness in separating oxygen, nitrogen, methane and carbon monoxide. Differently, the PLOTQ column (Col1) has been developed for the separation of targeted apolar and polar compounds including hydrocarbon (natural gas, refinery gas, ethylene, propylene and C1-C3 isomers), CO₂, methane, air/CO, water, polar solvents (methanol, acetone, methylene chloride, alcohols, ketones, aldehydes, esters) and sulfur compounds (H₂S, mercaptans, COS). During operating conditions, *valve1* is always set on “OFF” position while *valve2*, at a certain time, needs to switch from the “OFF” to the “ON” position (Fig. 4a and 4b) and then, again, to the original “OFF” position (Fig. 4a). These two configurations are necessary both to avoid the contamination of the Molsieve columns from unwanted components and to allow the Molsieve columns separation of the light and inert gases. For example, when a sample containing CO₂, Ar, O₂ and N₂ arrives at position n.5 of *valve1* (see Fig. 4a) the configuration of the GC circuit is the one shown in Fig. 4a. When crossed by this sample, the PlotQ column releases firstly Ar, O₂ and N₂ and, after a specific retention time, it releases CO₂. Ar, O₂ and N₂, not yet separated, enter Col2 and Col3 to allow the separation of these gases (Fig. 4a). Then, immediately before CO₂ reaches position n.5 of *valve2*, this valve switches to the “ON” position (Fig. 4b) in order to allow CO₂ to by-pass Col2 and Col3. Once CO₂ has by-

passed the series of Col2 and Col3, valve2 is switched to the “OFF” position (Fig. 4a) so that light gases, separated by the Molsieve columns, can reach the GC’s Thermal Conductivity Detector.

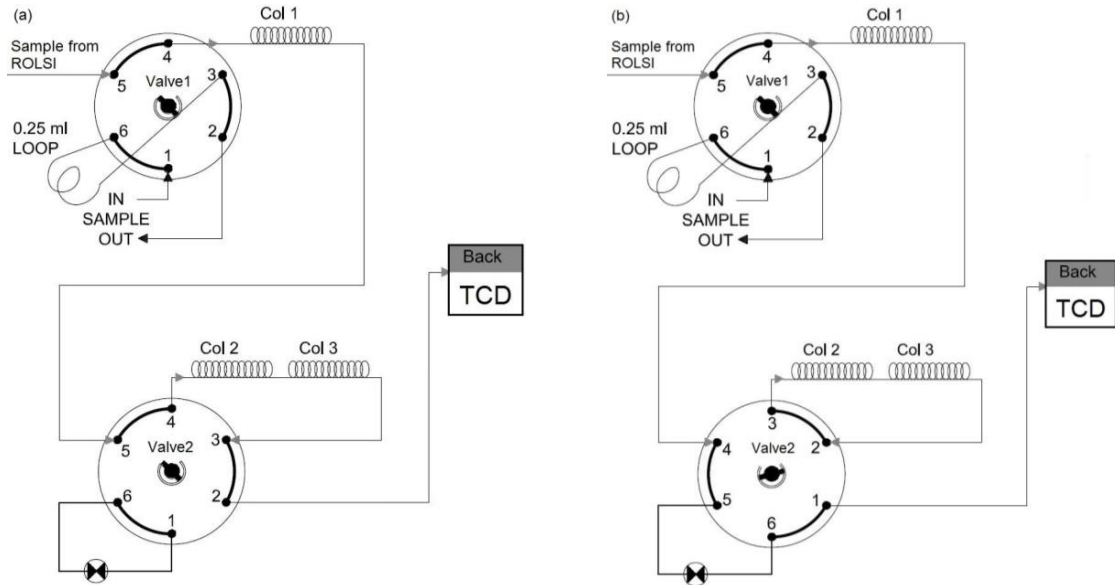


Fig. 4. Gas chromatograph column set up (a) valves in “OFF” position; (b) valve1 in “OFF” position and valve2 in “ON” position)

In chromatography, the area subtended by each i -th chromatogram peak depends on the amount of moles of the specific i -th component, n_i , which reaches the GC detector. The molar fraction x_i of each component of the mixture can be derived from:

$$x_i = n_i / \sum_{j=1}^N n_j \quad (i=1, \dots, N)$$

once:

- the area of each peak of the chromatogram is measured;
- the calibration function, which relates the number of moles detected by the GC to the area subtended by the relative chromatogram peak, is defined for each component.

The most important step in chromatography is the calibration of the GC, that consists of the definition of the mentioned calibration models for each component of the analysed mixture.

The GC has been equipped with an injector to allow the gas chromatograph calibration (see Fig. 1 to view the connection between GC and the two ROLSI). In fact, each calibration curve must be obtained by injecting known volumes of each component into the GC with syringes characterized by volumes of 5 – 500 μl . In particular, the number of injected moles is computed from the knowledge of the syringe volume and the derivation of the density as a function of measured ambient pressure and temperature. Models implemented in REFPROP[®] are used to calculate densities.

Unlike pressure and temperature measurements, the uncertainty in measured mole fraction of each species $u(x_i)$ depends on the system being considered. In fact, since mole fractions depend on the number of moles of each of the N components of the mixture, their uncertainty is calculated by combining different contributions:

$$u^2(x_i) = \sum_{j=1}^N \left\{ \left(\frac{\partial x_i}{\partial n_j} \right)^2 u^2(n_j) \right\} \quad (i=1, \dots, N)$$

In particular, since the derived number of moles n_j depends both on the measured area subtending each peak and on the calibration model, the uncertainty $u(n_j)$ is evaluated considering the estimated standard deviation of the mean area $A_{i,m}$, $u(A_{i,m})$, and the uncertainties which affect the calibration models. The former contribution, $u(A_{i,m})$, is estimated by considering five measurements for each calibration point. The latter source of error is strictly related to the uncertainty $u(n_{ref,j})$ of the estimated number of moles of each component introduced through syringes and considered as a reference during the calibrations. More specifically, $u(n_{ref,j})$ is computed by evaluating:

- the uncertainty of the syringe volume $u(V_{syr})$, declared by the manufacturer;
- the uncertainty of measured pressure P and temperature T , $u(P)$ and $u(T)$, used to evaluate density;
- the uncertainty of the thermodynamic model used to calculate density, declared by REFPROP, $u(\rho_{mod})$;

Hence, $u(n_j)$ is derived from the following expression:

$$u^2(n_j) = \left(\frac{\partial n_j}{\partial A}\right)^2 u^2(A_{i,m}) + \left(\frac{\partial n_{ref,j}}{\partial V}\right)^2 u^2(V_{syr}) + \left(\frac{\partial n_{ref,j}}{\partial P}\right)^2 u^2(P) + \left(\frac{\partial n_{ref,j}}{\partial T}\right)^2 u^2(T) + \left(\frac{\partial n_{ref,j}}{\partial \rho}\right)^2 u^2(\rho_{mod})$$

The calibration procedure also consists of setting the two characteristic sampling times $t1$ and $t2$ (see section 2.1) and the commutation time of the GC valve 2. Time $t1$ is set higher than the time required to separate the products inside columns. Time $t2$ is adjusted from 0.05 ms to 1 s, depending on the studied system and on the desired withdrawn amount of the sample.

4. Experimental procedure

The main objective of these measurements is to extract VLE isothermal phase diagrams for the binary mixture of interest. In particular, phase diagrams are obtained by first introducing into the cell the less volatile component and then by progressively increasing the pressure by introducing the second component. For each pressure level the composition of vapour and liquid phase is measured and a phase diagram is obtained.

This section details the procedure followed to carry out such measurements for binary mixtures, with the apparatus described above.

4.1. Preliminary operations

Before starting the operating procedure, it is necessary to set the following parameters:

- temperature of the ROLSI, T_R (usually set to 90°C);
- temperature of the sample transfer line ($T_R+10^\circ\text{C}$);
- temperature of the cell pressure transducers mounting (coincident with the calibration temperature);
- temperature of the gas tanks pressure transducer mounting (coincident with the calibration temperature);

A further preliminary step consists of setting the thermostatic bath temperature at the value dictated by the isotherm under study. During the bath temperature stabilization, the vacuum should be created in the whole measurement and loading circuits, to allow the filling of pure components inside the cell.

4.2. Measuring procedure

With the cell inside the bath, the first and less volatile component can be introduced. Once the bath has reached a stable thermal regime, the cell should be lifted out of the bath in order to check the achievement of a vapour-liquid equilibrium inside the cell volume. Then, the cell should be re-immersed waiting for thermal stability. Also, the set bath temperature should be adjusted until the temperature values recorded by the sensors inside the cell show the achievement of the desired temperature. At equilibrium, pressure and temperature are measured and samples of both the phases are withdrawn and analysed. Three samples of both liquid and vapour phases must be extracted from the two ROLSI to clean their capillaries from the presence of residual air. If air is effectively absent from the cell, next

samples should show only the presence of the first pure component. The first point (1) of the phase diagram (see Fig. 5 point 1) has been acquired (with reference to Fig. 5 $x_{\text{CO}_2}=100\%$).

Afterwards, the vacuum should be done in all the loading circuit, up to the inlet valves of the cell. A small fraction of the second component can be therefore introduced, leading to an increase in pressure. When pressure has stabilized, after the extraction of three samples from liquid and vapour ROLSI to clean the capillaries, five samples are withdrawn and analysed for each phase. Averaging the five composition measurements for each phase, bubble and dew points at the new pressure level are obtained (2L and 2V in Fig. 5).

Proceeding similarly, by progressively introducing the second component and recording pressure, temperature and liquid and vapour phases composition at each step, the whole phase diagram is obtained.

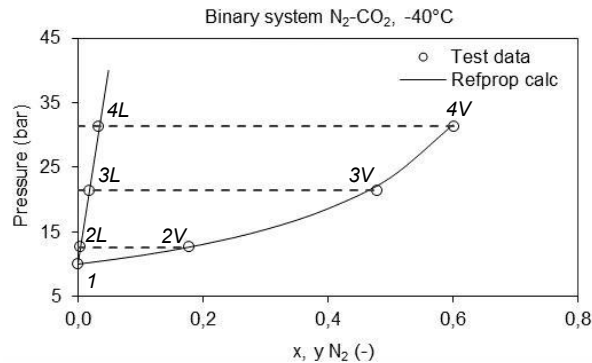


Fig. 5. Example of an extracted phase diagram

5. Data analysis

The measured variables in VLE mixtures are the liquid and vapour molar fractions of each component i (x_i and y_i), temperature T and pressure P . From the celebrated phase rule of J.W. Gibbs [12], it can be derived that, for a multicomponent non-reacting system in vapour-liquid equilibrium, the number of independent variables that must be fixed to establish its intensive state coincides with the number of components of the system. For example, in the case of a binary mixture ($i=2$) in vapour-liquid equilibrium and subjected to an isothermal increase of pressure, to any pair of measured T and x_i it is possible to derive P and y_i by applying *Bubble Pressure Calculation* methods [12, 25]. The derived fundamental criterion for phase equilibrium states that when multiple phases at the same P and T are in equilibrium, the chemical potential of each species is the same in all phases. To facilitate the application of equilibrium criteria to vapour (V) – liquid (L) equilibrium calculations, the fugacity is used in place of the chemical potential [12].

In general, results of VLE calculations mostly depend on the model used to express the fugacity in terms of pressure, temperature and phases composition. Two methods are applied for representing these relationships, the equation-of-state method and the activity coefficient method. The equation-of-state method derives all properties of both phases from an equation of state, while the activity coefficient method applies different models for the evaluation of liquid and vapour phase properties. In fact, while vapour phase properties are still derived from an equation of state, properties of liquid phases are obtained by summing properties of pure components and including a mixing or an excess term. Most of these models contain semi-empirical parameters which need to be regressed by minimizing the Mean Squared Error (MSE) between model predictions and experimental data obtained from the apparatus presented through this paper. More details can be found in [12]. Also, statistical analysis of residuals is carried out [26]. When experimental data are analysed, different models are considered and a comparison between results is performed. Furthermore, the applied data consistency tests are the point test and the direct test proposed by Van Ness [25, 27].

6. Conclusions

The test rig installed at LEAP enables the extraction of reliable experimental data for vapour – liquid equilibrium measurements in a small volume equilibrium cell, within the pressure and temperature ranges of 0 – 20 MPa and -60 – 200 °C. At present, the focus of the experimental activity is on studying the thermodynamics of mixtures for CO₂ capture and storage applications and of advanced working fluids for closed power cycles such as organic Rankine cycles and supercritical closed-cycle gas turbines.

Acknowledgements

The authors would like to thank “Fondazione Piacenza e Vigevano” for contributing to the realization of the VLE apparatus.

References

- [1] Invernizzi C. Closed Power Cycle: Thermodynamic Fundamentals and Applications. London: Springer-Verlag; 2013.
- [2] Angelino G. Real gas effects in carbon dioxide cycles. ASME Paper 69-GT-102
- [3] Angelino G. Perspectives for the Liquid Phase Compression Gas Turbine. Journal of Engineering for Power, Trans. ASME; April 1967; Vol. 89, No. 2: 229-237
- [4] Angelino G. Carbon Dioxide Condensation Cycles for Power Production. ASME Paper 1968; No. 68-GT-23.
- [5] Angelino G. Real Gas Effects in Carbon Dioxide Cycles. ASME Paper 1969; No. 69-GT-103.
- [6] Feher EG. The supercritical thermodynamic power cycle. Advances in Energy Conversion Engineering. Intersociety Energy Conversion Engineering Conference 1967.
- [7] Ma Z, Turchi CS, Advanced Supercritical Carbon Dioxide Power Cycle Configurations for Use in Concentrating Solar Power Systems. Supercritical CO₂ Power Cycle Symposium 2011.
- [8] Angelino G, Colonna di Paliano P. Multicomponent working fluids for organic Rankine cycles (ORCs). Energy 1998; 23: 449 - 463.
- [9] Invernizzi C, Van der Stelt T. Supercritical and real gas Brayton cycles operating with mixtures of carbon dioxide and hydrocarbons. Proceedings of the Institution of Mechanical Engineers, Part A: Journal of Power and Energy 2012; 226; 5: 682 - 693.
- [10] Visser E, et al.. Dynamis CO₂ quality recommendations. International Journal of Greenhouse Gas Control 2008; 2:478-487.
- [11] Li H, et al.. PVTxy properties of CO₂ mixtures relevant for CO₂ capture, transport and storage: Review of available experimental data and theoretical models. Applied Energy 2011; 88: 3567-3579.
- [12] Smith JM, Van Ness HC, Abbott MM. Introduction to Chemical Engineering Thermodynamics, 7th edition. New York: McGraw-Hill; 2005
- [13] Valenti G, et al. Pressure-volume-temperature measurements of CO₂-N₂-O₂ mixtures from -10°C to 150°C and from vacuum to 200 bar: description of the experimental apparatus based on a vibrating tube densimeter, atti del "63° Congresso Nazionale ATI (Associazione Termotecnica Italiana)", Palermo, Settembre 2008.
- [14] Mantovani M, et al.. P-p-T Measurements of CO₂-N₂ Mixtures in Supercritical Conditions, atti del "65° Congresso Nazionale ATI (Associazione Termotecnica Italiana)", Domus de Maria (CA), Settembre 2010.
- [15] Mantovani M, et al.. Supercritical pressure–density–temperature measurements on CO₂-N₂, CO₂-O₂ and CO₂-Ar binary mixtures, The Journal of Supercritical Fluids, Volume 61, Pages 34-43, Gennaio 2012
- [16] Mantovani M. Oxy-Combustion Flue Gases Purification Systems: Numerical and Experimental Analysis. Milano : s.n., 2010.
- [17] Mazzoccoli M. Carbon Capture, Storage and Transportation (CCS&T) Process: General Aspects and Focus on CO₂ Pipeline Modelling. Genova : s.n., 2011.
- [18] Morgan DI, Kobayashi R. Direct vapor pressure measurements of ten n-alkanes in the 10-C28 range. Fluid Phase Equilibria 1994; 97: 211 – 242.
- [19] Di Nicola G, et al.. Vapor–Liquid–Equilibrium (VLE) properties of R-32+R-134a system derived from isochoric measurements. Fluid Phase Equilibria 1998; 153: 143 -165.
- [20] Baba-Ahmed A, et al.. New equipment using a static analytic method for the study of vapour–liquid equilibria at temperatures down to 77K. Fluid Phase Equilibria 1999; 166: 225–236.
- [21] Courtial X, et al.. Vapor-liquid equilibrium in the n-butane + methanol system, measurement and modeling from 323.2 to 443.2 K. Fluid Phase Equilibria 2009; 277: 152–161.
- [22] Narasigadu C, et al.. A novel static analytical apparatus for phase equilibrium measurements. Fluid Phase Equilibria 2013; 338: 188-196.
- [23] Guilbot P, et al.. Rapid on-line sampler-injector: a reliable tool for HT-HP sampling and on-line GC analysis. Analisis 2000; 28: 426-431.
- [24] ENV 13005 - Guide to the expression of uncertainty in measurement. U ENV - UNI-CEI Metrologia Generale, Italy; 2000
- [25] Van Ness CH. Thermodynamics in the treatment of vapor/liquid equilibrium (VLE) data. Pure & Appl. Chem. 1995; 67: 859-872
- [26] Wisniak J, Polishuk A. Analysis of residuals - a useful tool for phase equilibrium data analysis. Fluid Phase Equilibria 1999; 164: 61–82
- [27] Van Ness HC, Byer SM, Gibbs RE. Vapor-Liquid equilibrium: Part I. An appraisal of data reduction methods. AIChE J. 1973; 19: 238-244